

Supramolecular Organisation of Polymeric Coordination Chains into a Three-Dimensional Network with Nanosized Channels that Clathrate Large Organic Molecules

Xian-Ming Zhang,^[a,b] Ming-Liang Tong,^[a] Meng-Lian Gong,^[a] and Xiao-Ming Chen^{*[a]}

Keywords: Coordination polymers / Microporous materials / Inclusion compounds / Supramolecular chemistry

Hydrothermal treatment of a mixture of $[\text{Zn}(\text{MeCO}_2)_2] \cdot \text{H}_2\text{O}$, terephthalic acid, and 2,2'-bipyridine resulted in a coordination polymer $[\text{Zn}(\text{bpy})(\text{tp})](\text{bpy})$ (**1**; bpy = 2,2'-bipyridine, H_2tp = terephthalic acid) which crystallizes in the monoclinic space group $C2/c$, $M_r = 541.85$, $a = 15.388(11)$, $b = 21.963(11)$, $c = 7.670(8)$ Å, $\beta = 112.82(2)^\circ$, $V = 2387(3)$ Å³, $Z = 4$, $D_c = 1.506$ g·cm⁻³. An X-ray single-crystal structural analysis reveals that **1** is a three-dimensional network with nanosized

channels constructed from one-dimensional coordination chains via C–H...O hydrogen bonds and aromatic intercalations. TGA and XRPD showed that the porous network of **1** is very stable while the guest 2,2'-bipyridine molecules in the channels are removable. Compound **1** shows a strong ligand-centred emission at room temperature in the solid state.

(© Wiley-VCH Verlag GmbH & Co. KGaA, 69451 Weinheim, Germany, 2003)

Introduction

Microporous inorganic materials including zeolites, aluminium phosphates, and transition metal phosphates are particularly important for their applications as molecular sieves, desiccants, ion exchangers, and catalysts,^[1–7] and thus they have been studied in detail in the past decades. Several years ago, microporous compounds were extended to pure organic and metal-organic frameworks, or coordination polymers.^[8–20] Compared with inorganic compounds, organic and coordination polymers built from molecular building blocks hold great promise for their ease of processability, flexibility, structural diversity, and geometrical control, such as the size, shape, and symmetry.^[12] However, most pure organic and coordination polymers do not possess a porous structure because of the interpenetration of two or more independent networks and the collapse of the network in the absence of guest molecules.^[21] Thus, the designed construction of extended porous organic or metal-organic frameworks from molecular building blocks is one of the most challenging issues in current synthetic chemistry.

Recent progress in the design and synthesis of porous metal-organic frameworks has been recently made by Yaghi, Williams, Kitagawa, and their co-workers, in particular, using the concept of secondary building units

(SBUs) for understanding and predicting the topologies of structures.^[12] The terephthalate (tp) anion is one of the best ligands for the design and construction of inorganic-organic hybrid porous frameworks owing to its thermal stability and symmetry. Hong and co-workers^[22] recently attempted to construct a porous coordination polymer with mixed tp and 1,10-phenanthroline (phen) ligands via aromatic π - π stacking interactions, but, due to the ill-suited orientation of the phen and tp groups, and the existence of coordinated water molecules, the networks obtained were not porous. From entropic and kinetic points of view, it is advantageous to arrange the building blocks in a more orderly fashion and remove the coordinated water molecules by reaction at higher temperatures and for longer times.^[8] We report here a new porous compound $[\text{Zn}(\text{bpy})(\text{tp})](\text{bpy})$ (**1**) generated by a high temperature hydrothermal reaction, which is constructed from infinite zigzag coordination polymeric chains via C–H...O hydrogen bonds and aromatic π - π stacking interactions.

Results and Discussion

Synthesis and Characterization

While well established for the syntheses of zeolites, the hydrothermal method has more recently been adapted to the preparation of complexes. There are a variety of hydrothermal parameters such as reaction time, temperature, pH value, and molar ratio of reactants, and small changes in one or more of the parameters may have a profound influence on the final reaction outcome. Compared with typical hydrothermal conditions for the synthesis of coordination

^[a] School of Chemistry and Chemical Engineering Sun Yat-Sen University Guangzhou 510275, China
Fax: (internat.) +86-20/8411-2245
E-mail: cesxcm@zsu.edu.cn

^[b] Department of Chemistry Shanxi Teachers University Linfen Shanxi 041004, China

polymers (120–180 °C and 2–7 days), compound **1** was synthesized at a higher reaction temperature (200 °C) during an exceptionally long reaction time (25 days).

Description of Crystal Structure

X-ray crystallography reveals that **1** consists of one-dimensional zigzag $[\text{Zn}(\text{bpy})(\text{tp})]_n$ chains and free bpy groups. There are 0.5 zinc atoms, and 0.5 tp, 0.5 coordinated bpy and 0.5 free bpy ligands in each asymmetric unit. The zinc atom in **1** has a highly distorted octahedral coordination environment with four oxygen atoms $[\text{Zn}(1)–\text{O}(1)$ 2.380(4), $\text{Zn}(1)–\text{O}(2)$ 2.057(4) Å, $\text{O}(1)–\text{Zn}(1)–\text{O}(2)$ 59.3(2)°] from two tp groups and two nitrogen atoms $[\text{Zn}(1)–\text{N}(1)$ 2.132(4) Å and $\text{N}(1)–\text{Zn}(1)–\text{N}(1a)$ 77.2(2)°] from a chelating bpy ligand, as shown in Figure 1. Each tp group acts in a bis-bidentate mode and bridges two zinc atoms, resulting in $[\text{Zn}(\text{bpy})(\text{tp})]_n$ chains with additional bpy ligands found alternately on both sides. The $\text{Zn}\cdots\text{Zn}\cdots\text{Zn}$ angle formed by three adjacent zinc atoms is 128°. Both carboxylate ends function in an asymmetric chelate mode, as evidenced by the $\text{Zn}(1)–\text{O}(1)$ and $\text{Zn}(1)–\text{O}(2)$ bond lengths.

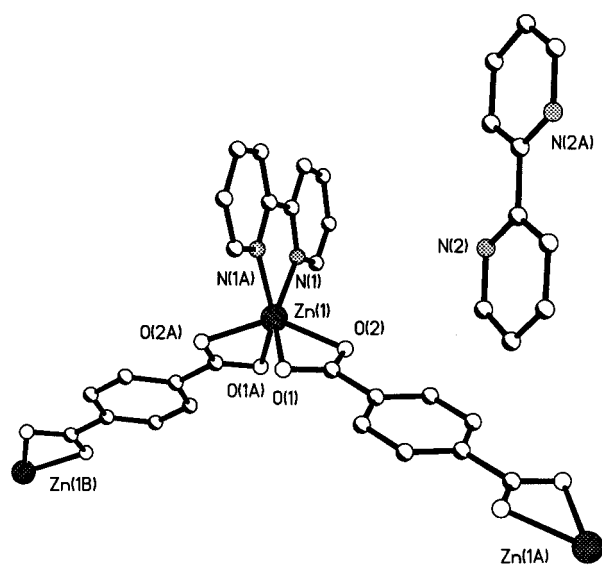


Figure 1. Perspective view of the coordination environment of the zinc atom and the guest bpy molecule in **1**

Two strong bands at 1563 (s) and 1395 (s) cm^{-1} in the IR spectrum are due to the antisymmetric and symmetric stretching vibrations of the carboxylate group, respectively. The difference ($\Delta = 168 \text{ cm}^{-1}$) between $\nu_{\text{asym}}(\text{CO}_2)$ and $\nu_{\text{sym}}(\text{CO}_2)$ is similar to that of an ionic carboxylate, which may be attributed to existence of the $\text{C}–\text{H}\cdots\text{O}$ hydrogen bond associated with the carboxylate oxygen atoms (see below), hence the carboxylate end behaves like a bridging carboxylate- O, O' group in the IR spectrum of **1**.

It should be noted that there are persistent one-dimensional $\text{C}–\text{H}\cdots\text{O}$ hydrogen bond interactions between adjacent $[\text{Zn}(\text{bpy})(\text{tp})]_n$ chains. Recent studies^[23] have revealed that the $\text{C}\cdots\text{O}$ distance (D) in $\text{C}–\text{H}\cdots\text{O}$ hydrogen bond is

in the range of 3.0–4.0 Å. The $\text{C}–\text{H}\cdots\text{O}$ angle θ in the range of 110–180° is acceptable, although a linear $\text{C}–\text{H}\cdots\text{O}$ bond ($150^\circ < \theta < 180^\circ$) is structurally more important. In **1** the $\text{C}(3)\cdots\text{O}(1)$ distance of 3.489 Å and $\text{C}(3)–\text{H}(3a)\cdots\text{O}(1)$ angle of 157.3° indicate a strong $\text{C}–\text{H}\cdots\text{O}$ hydrogen bond. Two complementary $\text{C}–\text{H}\cdots\text{O}$ hydrogen bonds form a double-linked $\text{C}–\text{H}\cdots\text{O}$ hydrogen bond interaction which further extends the $[\text{Zn}(\text{bpy})(\text{tp})]_n$ chains into undulating $[\text{Zn}(\text{bpy})(\text{tp})]_n$ layers, as shown in Figure 2a. Within the layer, the separation between two adjacent bpy ligands is ca. 7.0 Å. Hydrogen bond interactions are usually important in the synthesis of supramolecular architectures,^[24] and in **1** they undoubtedly play an important role in the stabilization of the layer structure and the control of the orientation of the tp ligands. Besides the $\text{C}–\text{H}\cdots\text{O}$ hydrogen bond, the pyridyl C(8) [with H(8a)] atom also forms a hydrogen bond with the carboxy O(2) atom from an adjacent layer, in which the $\text{C}(8)\cdots\text{O}(2)$ distance and $\text{C}(8)–\text{H}(8a)\cdots\text{O}(2)$ angle are 3.254 Å and 129.3°, respectively (Figure 2b).

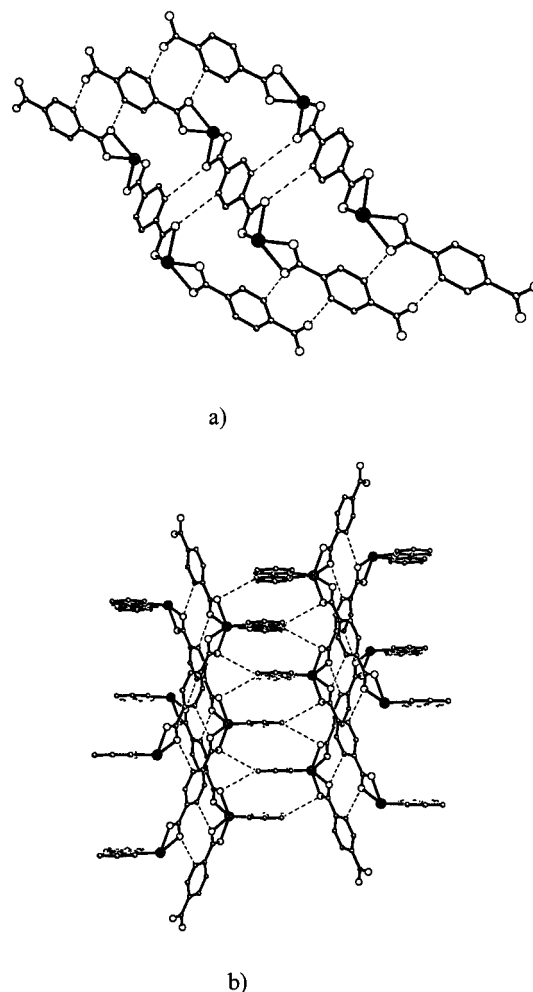


Figure 2. Perspective views of the two-dimensional layers constructed by the zigzag chains and $\text{C}–\text{H}\cdots\text{O}$ hydrogen bonds: (a) top-view of a single layer; (b) side-view of two layers exhibiting the intercalation of the lateral bpy ligands

Aromatic π - π stacking interactions are also apparent in **1**, as shown in Figure 2b. Aromatic π - π stacking interactions can be depicted by centroid-centroid distance, plane-to-plane distance, and displacement angle.^[25] The displacement angle means the angle formed between the ring-centroid vector and the ring normal to one of the pyridine planes. In **1**, the centroid-centroid distance (3.85 Å) between two coordinated pyridine fragments, plane-to-plane distance (3.46 Å) and displacement angle (26°) indicate strong π - π stacking interactions between adjacent bpy ligands. All lateral bpy ligands from adjacent undulating $[\text{Zn}(\text{bpy})(\text{tp})]_n$ layers are parallel-displaced and intercalated in a zipper-like mode similar to some previously documented examples,^[26] which, in combination with the C(8)–H(8a)···O(2) hydrogen bond, further extends the undulating layers into a three-dimensional supramolecular network featuring one-dimensional nanosized saddle-like channels running along the *c* axis (Figure 3). The guest bpy molecules reside in the channels and exhibit an intermolecular parallel-displaced stacking geometry (plane-to-plane distance 3.5 Å) between themselves. Although the three-dimensional structure of **1** is somewhat similar to that of $[\text{Cu}(4,7\text{-phen})_2(\text{H}_2\text{O})_3](\text{ClO}_4)_2 \cdot (4,7\text{-phen})_2$,^[27] it is, in fact, constructed in a significantly different fashion. The three-dimensional architecture of this copper compound is formed by the parallel stacking of adjacent S-shaped “triple chains”; in contrast, that of **1** is formed by the zipper-like intercalation of the lateral bpy ligands.

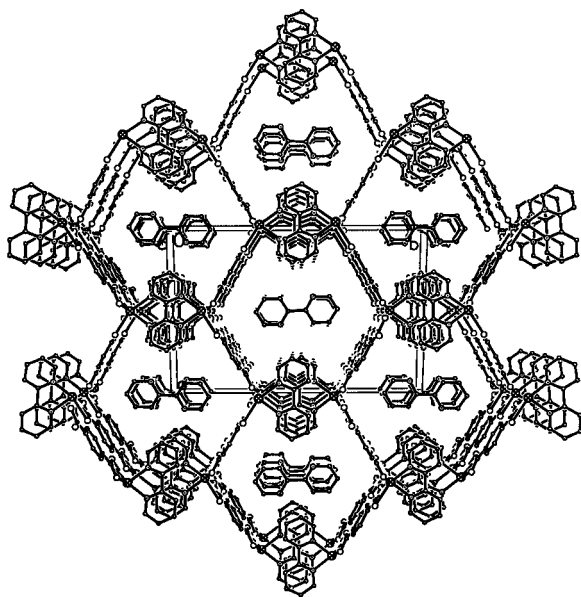


Figure 3. Perspective view of the three-dimensional network along the *c* axis

It is worthwhile to note that the free dimensions (13×7 Å) of these channels produced after calcination of **1** occupy as much as 40.7% of the crystal volume,^[28,29] a figure similar to those of $[\text{Cu}_3(\text{TMA})_2(\text{H}_2\text{O})_3]$ ^[8] and $[\text{Zn}_2(\text{BTC})(\text{NO}_3)](\text{H}_2\text{O})(\text{EtOH})_5$ ^[30] (41% and 43.6%, re-

spectively) and those (47% to 50%) of the most open zeolites, such as the faujasite, paulingite, and zeolite A families.^[2] In the formation of the channels in **1**, the C–H···O hydrogen bonds play a critical role because they make the tp ligands arranged in an orderly fashion, which minimizes the volume occupied by the network skeleton by controlling the orientation of the tp building blocks, leaving the large one-dimensional channels that are occupied by the guest bpy molecules.

In order to study the microporosity chemistry of **1**, thermogravimetric analysis (TGA) was performed in air and at 1 atm. pressure at a heating rate of $10^\circ\text{C}\cdot\text{min}^{-1}$ on a polycrystalline sample of this material, which showed the following clear and well-separated weight loss steps. As shown in Figure 4, a total weight loss of 29.0% occurred over the temperature range 190–310 °C, corresponding to the removal of one free bpy molecule per formula unit (calcd. 28.8%), followed by a two-step total weight loss of 56.3% between 340 and 640 °C consistent with the removal of coordinated bpy and tp ligands. The remaining weight of 14.7% corresponds to the percentage (15.0%) of the Zn and O components, indicating that the final product is ZnO. It should be noted that no weight loss was observed in the temperature range 310–340 °C. Therefore the TGA curve of **1** indicates that: 1) the free bpy molecules are removed from the channels in the temperature range 190–310 °C, whereas the coordinated bpy and tp ligands do not decompose over this temperature range; 2) in air and under 1 atm. pressure, a phase formulated as $[\text{Zn}(\text{bpy})(\text{tp})]$ is stable in the temperature range 310–340 °C, which is unusually high for a one-dimensional coordination polymer.

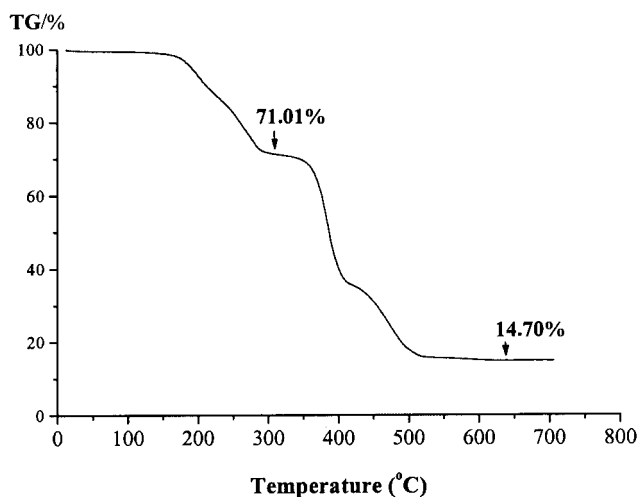


Figure 4. Thermogravimetric analysis curve of **1**

The above conclusions have also been supported by calcination of **1**. Elemental microanalysis (C 56.05, H 3.14, N 7.26) of **1** after calcination (designated as **1'**) in air at 220 °C and 10^{-2} Torr for 10 hours shows that the free bpy molecules are removed in the course of calcination. The X-ray powder diffraction patterns (Figure 5) of **1** and **1'** are similar while the positions, intensities and widths of some

peaks show minor differences, thus indicating that the porous network of **1** is retained after the calcination and removal of guests.

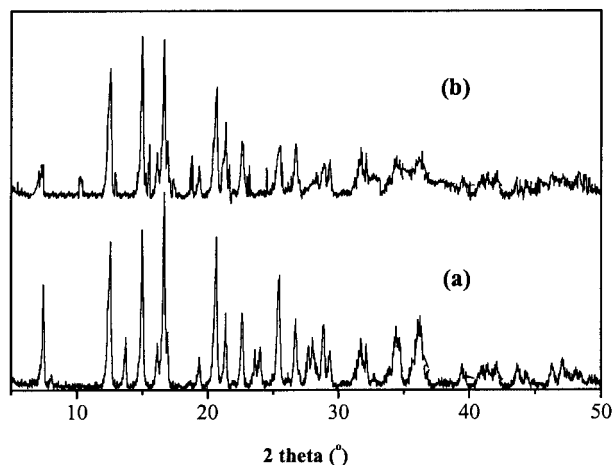


Figure 5. The XRPD patterns for: (a) as-synthesized **1** with bpy in the channels, and (b) the calcinated material

Photoluminescence

In the solid state, **1** shows an intense and broad emission band ranging from 400 to 600 nm upon photoexcitation ($\lambda_{\text{ex}} = 260$ nm; Figure 6). The maxima of the emission bands are located at 468 and 540 nm. According to the literature,^[31,32] the emission at 468 nm can be assigned to the $^1\pi, \pi^*$ state of the bpy ligands and the small shoulder at 540 nm to the $^1\pi, \pi^*$ state of free bpy molecules. The blue shift of the emission at 468 nm compared to that of free bpy ligand is possibly due to the fact that the bpy ligands are not allowed to relax along the inter-ring torsional mode upon photoexcitation.

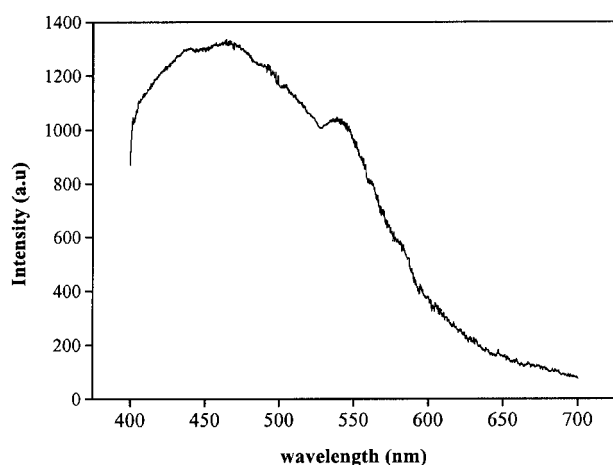


Figure 6. Photoluminescent spectrum of **1** excited at 260 nm

Experimental Section

General Remarks: Elemental analyses were performed on a Perkin–Elmer 240 elemental analyzer. The FT-IR spectra were re-

corded from KBr pellets between 400 and 4000 cm^{-1} on a Nicolet 5DX spectrometer. Thermal gravimetric analyses (TGA) were performed under a static air atmosphere using a Perkin–Elmer 7 thermogravimetric analyzer with a heating rate of 10 $^{\circ}\text{C}\cdot\text{min}^{-1}$. The XRPD patterns were recorded on a Rigaku D/Max 3III diffractometer with a scanning rate of 4 $\text{deg}\cdot\text{min}^{-1}$. Photoluminescence of **1** was performed at room temperature on a Hitachi F-4500 spectrometer.

Preparation of 1: A mixture of $\text{Zn}(\text{MeCO}_2)_2\cdot\text{H}_2\text{O}$ (0.112 g), H_2tp (0.083 g), NaOH (0.040 g), bpy (0.079 g), and water (10 mL) in a 1:1:2:1:1100 molar ratio was stirred for 20 min in air, then sealed in a 23 mL Teflon-lined stainless steel container, which was heated to 200 $^{\circ}\text{C}$ for 25 days. After cooling to room temperature at a rate of 5 $^{\circ}\text{C}$ per hour, pale-yellow large block crystals (ca. $3.2 \times 2.3 \times 1.5$ mm) of **1** were recovered in 60% yield based on bpy. $\text{C}_{28}\text{H}_{20}\text{N}_4\text{O}_4\text{Zn}$ (541.85): calcd. C 60.06, H 3.72, N 10.34; found C 59.87, H 3.81, N 10.26. IR (KBr): $\tilde{\nu} = 3436$ cm^{-1} m, 3069 w, 1563 s, 1443 m, 1395 s, 1294 m, 1174 w, 1018 w, 903 m, 842 s, 760 s, 546 m.

Preparation of the Porous Framework 1': Compound **1** was calcinated in a vacuum oven at 220 $^{\circ}\text{C}$ under a pressure of ca. 10^{-2} Torr for 10 h. $\text{C}_{18}\text{H}_{12}\text{N}_2\text{O}_4\text{Zn}$ (385.69): calcd. C 56.05, H 3.14, N 7.26; found C 55.94, H 3.07, N 7.21.

X-ray Crystallographic Study: Diffraction intensities were collected at 293 K on a Siemens R3 diffractometer ($\text{Mo-K}\alpha$, $\lambda = 0.71073$ Å). Lorentz-polarization and absorption corrections were applied. The structures were solved by direct methods (SHELXS-97)^[33] and refined by full-matrix least-squares techniques (SHELXL-97). Analytical expressions of neutral-atom scattering factors were employed, and anomalous dispersion corrections were incorporated. In all cases, all non-hydrogen atoms were refined anisotropically and hydrogen atoms of organic ligands were geometrically placed. The crystallographic data are listed in Table 1 and selected interatomic distances and angles are given in Table 2.

Table 1 Crystal and structure refinement for complex **1**

Empirical formula	$\text{C}_{28}\text{H}_{20}\text{N}_4\text{O}_4\text{Zn}$
Formula weight	541.85
Temperature [K]	293(2)
Wavelength [Å]	0.71073
Crystal system	monoclinic
Space group	$C2/c$
a [Å]	15.388(11)
b [Å]	21.963(11)
c [Å]	7.670(8)
β [°]	112.82(2)
V [Å ³]	2389(3)
Z	4
Density [Mg/m^3]	1.506
Absorption coefficient [mm^{-1}]	1.072
$F(000)$	1112
No. indep. refl.	2100
No. obs. refl.	1662
Data/restraints/parameters	2100/0/169
Goodness-of-fit on F^2	1.084
R_1 [$I > 2\sigma(I)$]	0.0603
wR_2	0.1741
Extinction coefficient	0.0039(9)
Largest diff. peak and hole [$\text{e}\cdot\text{Å}^{-3}$]	0.532 and -0.645

CCDC-173807 contains the supplementary crystallographic data for this paper. These data can be obtained free of charge at www.ccdc.cam.ac.uk/conts/retrieving.html [or from the Cambridge

Table 2. Selected bond lengths [Å] and angles [°] for **1**

Zn(1)–O(2)	2.057(4)	N(1a)1–Zn(1)–N(1)	77.2(2)
Zn(1)–N(1)	2.132(4)	O(2)–Zn(1)–O(1a) ^[a]	98.5(2)
Zn(1)–O(1)	2.380(4)	N(1)–Zn(1)–O(1a)	88.3(2)
		O(2)–Zn(1)–O(1)	59.3(2)
O(2a)–Zn(1)–O(2)	140.5(2)	N(1a)–Zn(1)–O(1)	88.3(2)
O(2)–Zn(1)–N(1a)	109.8(2)	N(1)–Zn(1)–O(1)	150.1(2)
O(2)–Zn(1)–N(1)	101.0(2)	O(1a)–Zn(1)–O(1)	115.2(2)

^[a] Symmetry code: a) $-x, y, -z + 1/2$.

Crystallographic Data Centre, 12, Union Road, Cambridge CB2 1EZ, UK; Fax: (internat.) +44–1223/336-033; E-mail: deposit@ccdc.cam.ac.uk].

Acknowledgments

This work was supported by the National Natural Science Foundation of China (No. 20131020 & 29971033) and the Ministry of Education of China (No. 01134).

- ^[1] A. K. Cheetham, G. Férey, T. Loiseau, *Angew. Chem. Int. Ed.* **1999**, *38*, 3268–3292.
- ^[2] D. W. Breck, *Zeolite Molecular Sieves*, Kreiger, Malabar, **1974**.
- ^[3] S. T. Wilson, B. M. Lok, C. A. Messina, T. R. Cannan, E. M. Flanigen, *J. Am. Chem. Soc.* **1982**, *104*, 1146–1147.
- ^[4] T. E. Gier, G. D. Stucky, *Nature* **1991**, *349*, 508–510.
- ^[5] M. E. Davis, *Acc. Chem. Res.* **1993**, *26*, 111–115.
- ^[6] T. E. Gier, X. Bu, P. Feng, G. D. Stucky, *Nature* **1998**, *395*, 154–157.
- ^[7] P. Feng, X. Bu, G. D. Stucky, *Nature* **1997**, *388*, 735–741.
- ^[8] S. S.-Y. Chui, S. M.-F. Lo, J. P. H. Charmant, A. G. Orpen, I. D. Williams, *Science* **1999**, *283*, 1148–1150.
- ^[9] L. Chen, M. Eddaoudi, S. T. Hyde, M. O'Keeffe, O. M. Yaghi, *Science* **2001**, *291*, 1021–1023.
- ^[10] S.-I. Noro, S. Kitagawa, M. Kondo, K. Seki, *Angew. Chem. Int. Ed.* **2000**, *39*, 2082–2084.
- ^[11] M. Eddaoudi, J. Kim, M. O'Keeffe, O. M. Yaghi, *J. Am. Chem. Soc.* **2002**, *124*, 376–377.
- ^[12] O. M. Yaghi, H.-L. Li, C. Davis, D. Richardson, T. L. Groy, *Acc. Chem. Res.* **1998**, *31*, 474–484.
- ^[13] H. K. Chae, M. Eddaoudi, J. Kim, S. I. Hauck, J. F. Hartwig, M. O'Keeffe, O. M. Yaghi, *J. Am. Chem. Soc.* **2001**, *123*, 11482–11483.
- ^[14] J. Kim, B. Chen, T. M. Reineke, H. Li, M. Eddaoudi, D. B. Moler, M. O'Keeffe, O. M. Yaghi, *J. Am. Chem. Soc.* **2001**, *123*, 8239–8247.
- ^[15] M. Eddaoudi, J. Kim, J. B. Wachter, H. K. Chae, M. O'Keeffe, O. M. Yaghi, *J. Am. Chem. Soc.* **2001**, *123*, 4368–4369.
- ^[16] H. Li, M. Eddaoudi, M. O'Keeffe, O. M. Yaghi, *Nature* **1999**, *402*, 276–279.
- ^[17] M. J. Zaworotko, *Angew. Chem. Int. Ed.* **2000**, *39*, 3052–3054.
- ^[18] K. Biradha, C. Seward, M. J. Zaworotko, *Angew. Chem. Int. Ed.* **1999**, *38*, 492–495.
- ^[19] K. Biradha, Y. H. Hongo, M. Fujita, *Angew. Chem. Int. Ed.* **2000**, *39*, 3843–3845.
- ^[20] M. Eddaoudi, D. B. Moler, H. Li, B. Chen, T. M. Reineke, M. O'Keeffe, O. M. Yaghi, *Acc. Chem. Res.* **2001**, *34*, 319–330.
- ^[21] S. R. Batten, R. Robson, *Angew. Chem. Int. Ed.* **1998**, *37*, 1460–1496.
- ^[22] D.-F. Sun, R. Cao, Y.-C. Liang, Q. Shi, W.-P. Su, M.-C. Hong, *J. Chem. Soc., Dalton Trans.* **2001**, 2335–2340.
- ^[23] G. R. Desiraju, *Acc. Chem. Res.* **1996**, *29*, 441–449.
- ^[24] M. J. Krische, J.-M. Lehn, *Struct. Bonding* **2000**, *96*, 3–29.
- ^[25] C. Janiak, *J. Chem. Soc., Dalton Trans.* **2000**, 3885–3896.
- ^[26] S.-L. Zheng, M.-L. Tong, R.-W. Fu, X.-M. Chen, S.W. Ng, *Inorg. Chem.* **2001**, *40*, 3562–3569.
- ^[27] M.-L. Tong, S.-L. Zheng, X.-M. Chen, T. Yuen, C. L. Lin, X.-Y. Huang, J. Li, *New J. Chem.* **2001**, 1482–1485.
- ^[28] The channel dimensions are estimated from the van der Waals radii for carbon (1.70 Å), nitrogen (1.55 Å), and oxygen (1.40 Å).
- ^[29] A. L. Spek, *PLATON, A Multipurpose Crystallographic Tool*, Utrecht University: Utrecht, The Netherlands, **1999**.
- ^[30] M. Yaghi, C. E. Davis, G. Li, H. Li, *J. Am. Chem. Soc.* **1997**, *119*, 2861–2868.
- ^[31] K. D. Ley, K. S. Schanze, *Coord. Chem. Rev.* **1998**, *171*, 287–307.
- ^[32] V. W. W. Yam, K. K. W. Lo, *Chem. Soc. Rev.* **1999**, *28*, 323–334.
- ^[33] G. M. Sheldrick, *SHELX-97, Program for X-ray Crystal Structure Solution and Refinement*, Göttingen University, Germany (**1997**).

Received June 20, 2002
[I02339]